

Remote sensing and photogrammetry techniques in diagnostics of concrete structures

Artur Janowski^{1,2a}, Krystyna Nagrodzka-Godycka^{*1}, Jakub Szulwic^{1b} and Patryk Ziółkowski^{1c}

¹Faculty of Civil and Environmental Engineering, Gdansk University of Technology, Gdansk, Poland

²Faculty of Geodesy, Geospatial and Civil Engineering, University of Warmia and Mazury, Olsztyn

(Received May 1, 2015, Revised March 29, 2016, Accepted March 30, 2016)

Abstract. Recently laser scanning technologies become widely used in many areas of the modern economy. In the following paper authors show a potential spectrum of use Terrestrial Laser Scanning (TLS) in diagnostics of reinforced concrete elements. Based on modes of failure analysis of reinforcement concrete beam authors describe downsides and advantages of adaptation of terrestrial laser scanning to this purpose, moreover reveal under which condition this technology might be used. Research studies were conducted by Faculty of Civil and Environmental Engineering at Gdansk University of Technology. An experiment involved bending of reinforced concrete beam, the process was registered by the terrestrial laser scanner. Reinforced concrete beam was deliberately overloaded and eventually failed by shear. Whole failure process was tracing and recording by scanner Leica ScanStation C10 and verified by synchronous photographic registration supported by digital photogrammetry methods. Obtained data were post-processed in Leica Cyclone (dedicated software) and MeshLab (program on GPL license). The main goal of this paper is to prove the effectiveness of TLS in diagnostics of reinforced concrete elements. Authors propose few methods and procedures to virtually reconstruct failure process, measure geometry and assess a condition of structure.

Keywords: beam; cracks; deformation measurement; modes of failure; reinforced concrete; terrestrial laser scanning

1. Introduction

A majority can say for sure that concrete is most common construction material in all sort of widely understood engineering structures. Since the first concrete structure has been built, properties of concrete materials and construction technology become remarkably diverse. Simultaneously our knowledge about phenomena occurring in concrete has expanded. Despite great efforts of many people, an inevitable fact is that concrete, as each material, decays by many

*Corresponding author, Professor, E-mail: krystyna.nagrodzka-godycka@pg.gda.pl

^aPh.D., E-mail: artur.janowski@pg.gda.pl

^bPh.D., E-mail: jakub.szulwic@pg.gda.pl

^cM.Sc. Eng., E-mail: patryk.ziolkowski@pg.gda.pl

factors, such as rheology, high temperature or chemical environmental exposure. Deterioration of concrete affects appearance and behaviour of the structure. Symptoms of poor concrete condition might be visible as enormous deflections or cracking. Cracks may stimulate corrosion of rebars and lead to loss of adhesion which consequence is a decline of load carrying capacity. In many cases, preservation measures can augment structure lifetime cycle by many years. Proper repair strategy should be based on accurate diagnostics and ongoing assessment of structural condition. Appropriate decisions made by stakeholders, based on real information of concrete condition can save money and reduce risk associated with an investment. Comprehensive analysis of concrete elements is widespread issue that has been described in literature (Bencardino *et al.* 2014, Godycki-Cwirko 1992, Kopanska *et al.* 2016, Nagrodzka-Godycka *et al.* 2014, Windisch 1998). In literature dealing with teardown analysis of reinforced concrete elements, also reference to the modern measurement methods, including methods of image analysis and laser scanning might be found (Daliga *et al.* 2016, Dias-da-Costa *et al.* 2014, Diego *et al.* 2008, Gordon *et al.* 2007, Koken *et al.* 2014, Kwak *et al.* 2013, Lichti *et al.* 2011, Olsen *et al.* 2010, Qi *et al.* 2014, Teza *et al.* 2009). The study presented in the paper, made by TLS and digital photogrammetry methods, focused on the visual assessment of reinforced concrete beam, in contrary to studies using eg. ultrasound to insight into internal concrete condition (Moradi-Marani *et al.* 2014, Rucka *et al.* 2013). The authors decided to evaluate the mode of failure, through analysis of cracks on a surface of reinforced concrete beams using TLS. Extended analysis and verification process of proposed methods based on the use of TLS were carried out with synchronous photography supported by photogrammetric solutions and computer vision. Previous research conducted by the authors (Janowski *et al.* 2014, Nagrodzka-Godycka *et al.* 2014) indicate the importance of photogrammetry and laser scanning data analysis (Janowski *et al.* 2013, Blaszcak-Bak *et al.* 2015) in an improvement of quality and accuracy improvement in reinforced concrete diagnostics. The approach described in this paper can be used not only for analysis of reinforced concrete beams but also for other structural elements as well, for study purposes test set-up was prepared.

2. Research object, environment

The paper presents an analysis of data from the registered overloading process of reinforced concrete beam (Fig. 1). Terrestrial laser scanner measurement was set up to gather as much



Fig. 1 Test set-up, beam located under hydraulic jack and prepared for measurement

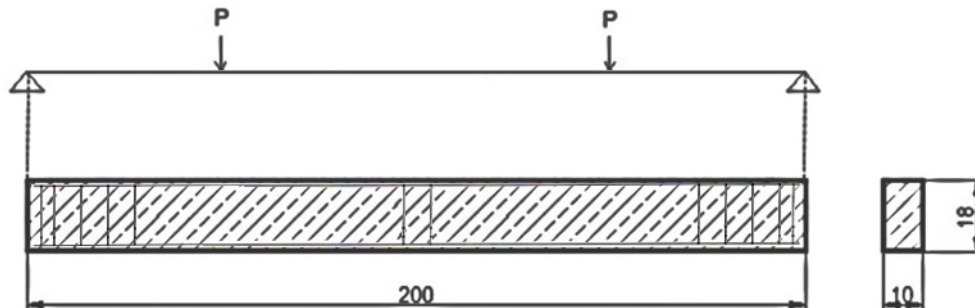


Fig. 2 Static scheme and schematic longitudinal and a transverse cross-section of the reinforced concrete beam.

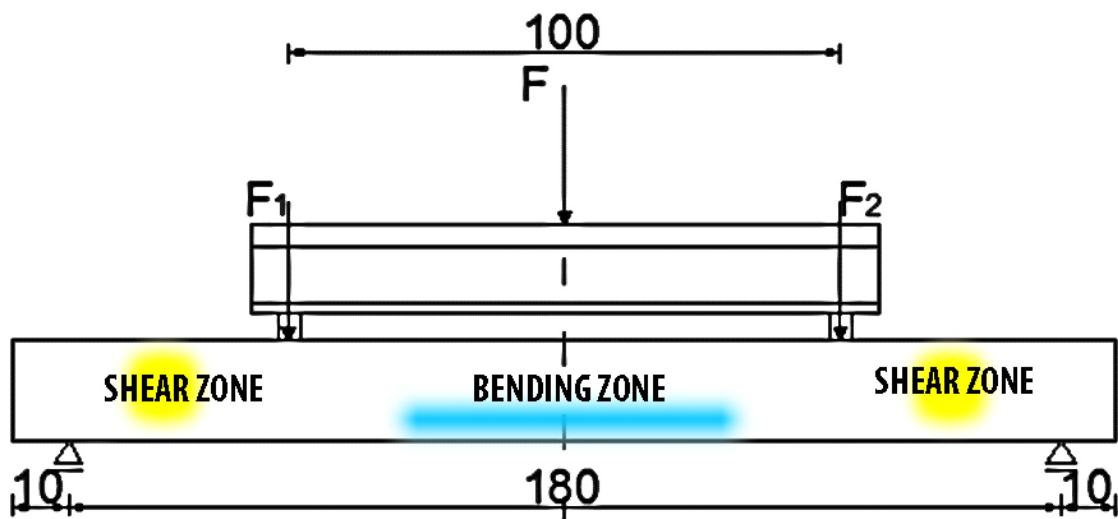


Fig. 3 Test set-up

information as possible from registered failure process. The beam was designed to fail by shear. In order to obtain an expected mode of the failure, the bending zone had strong longitudinal flexural reinforcement while shear zone had insufficient transverse reinforcement (Fig. 3), this action caused failure by shear. The beam was made of concrete C25/30 and reinforcing steel A-IIIIN. Schematic view of the beam is shown in Fig. 2, test set-up in Fig. 3.

Research have been carried out in the Regional Laboratory of Civil Engineering at Faculty of Civil and Environmental Engineering, Concrete Structure Department, at Gdansk University of Technology. Previously prepared concrete beam was installed in a special set-up by crane hoist. The whole configuration simulated static scheme assumed by authors, whereby the position of the beam was strictly set. To fulfil predefined condition, semi-circular steel supports and I-beam steel traverse were used to imitate hinged support and two symmetrically point loads. Load from the hydraulic stand was applied by I-beam steel traverse and two wooden pads in increments of 10kN

Table 1 The increase of load in the course of overloading (Legend: underline - failure load / *italic* – cracks occurrence)

	Stage 1 [kN]	Stage 2 [kN]	Stage 3 [kN]	Stage 4 [kN]	Stage 5 [kN]	Stage 6 [kN]	Stage 7 [kN]
Load	0.00	10.00	30.00	<i>50.00</i>	70.00	90.00	<u>140.70</u>

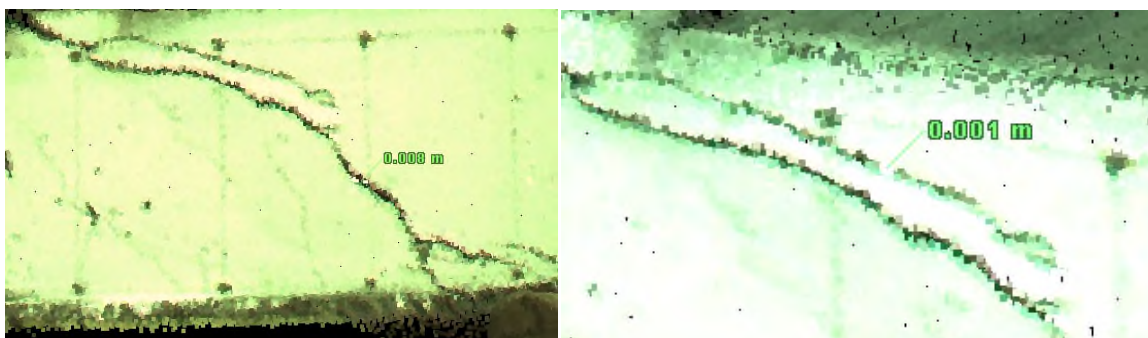


Fig. 4 View of reinforced concrete beam support in the Cyclone (stage 6, table 1). Measuring width of a cracks

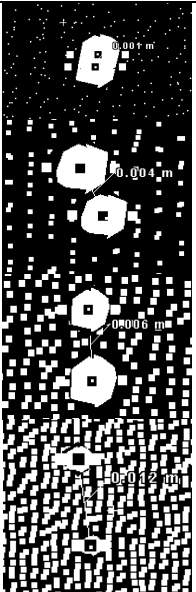
per stage until failure (Table 1). After each load increment, hydraulic stand was stopped and the beam was scanned by the terrestrial laser scanner. Surface morphology and crack growth have been controlled using Brinell Magnifier. Moreover, deflection control was provided by using dial deflectometer. For further studies, two synchronous cameras were used in order to make digital close range photogrammetry verification.

3. Data processing

The entire overloading process was captured by professional terrestrial laser scanner Leica ScanStation C10. ScanStation C10 belong to TLS genus, which gives an ability to the independent adjusting of horizontal and vertical resolution. This functionality allows to optimize scanning time and can be an asset during measurement held by terrestrial as well as mobile scanning (Burdziakowski *et al.* 2015, Nagrodzka-Godycka *et al.* 2014). To prevent an occurrence of crucial linking and matching correlation errors, the position of scanner did not change during the whole measurement process. Authors have made special preparations of lateral beam surface, engobed and grillage has been made with regular 100 mm rectangular grid. In tangle points of the plotted lines, circular tags with a diameter of 6 mm were deployed. Measurements were performed in two resolutions: medium (default) and predefined high (distance: 100.00 m; horizontal: 0.05 m; vertical: 0.01 m). Considering the close distance between object and scanner genuine resolution was even higher (horizontal: 0.0025 m; vertical 0.0005 m). Due to selecting higher resolution image detail has been improved in the post-processing stage. The medium resolution was characterized by less image detail. High resolution is significant to capture cracks occurrence (Fig. 4). The beam has been scanned along its entire length until it reaches failure by shear.

Data collected during the measurement were post-processed in program Cyclone provided by Leica Geosystems. Each sample has been placed in one unified coordinate system.

Table 2 Comparison of deflection values, measured directly using dial deflectometer and based on spheres position (Comparison of the results from model obtained by TLS and those by using measurements derived from synchronous images - according to the method described in Chapter 5)

Measurement epoch	Load [kN]	Deflection [mm]	Deflection in accordance with scan model / photogrammetry model measurements [mm]	Deflection value difference [mm]	Scan view
2	30.00	1.81	1.00 / 1.25	+0.81 / +0.56	
3	50.00	3.32	4.00 / 3.56	-0.68 / -0.24	
5	90.00	5.89	6.00 / 5.92	-0.11 / -0.03	
6	140.70	-	12.00 / 12.23	-	

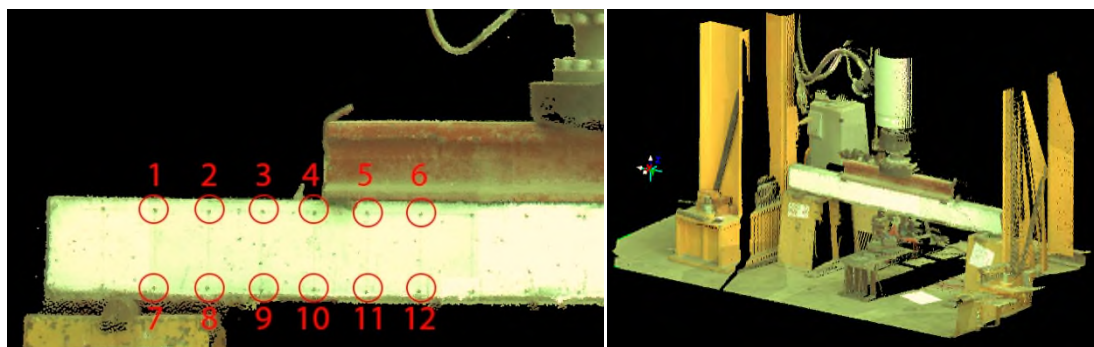


Fig. 5 View at measurement station and lateral surface of beam with marked characteristic points - 12 points were selected for analyses

4. Scanning data analysis methods

Proper analysis of measurement data was carried out in two programs. The first program was Cyclone which is dedicated software to operate with data from ScanStation C10 scanner. The second program was MeshLab, an open source and extensible system to work with the point cloud.

4.1 Spheres translation method

Method is based on a conversion of physical virtual tags mapping to a virtual spherical mesh object. In simpler terms method boils down to selecting characteristic points in point cloud model, in the case of these studies, markers were presented in the form of discs with 6mm diameter previously placed on the lateral surface of the beam (Fig. 5). After registration (scanning), followed by mapping for subsequent stages of the beam load, points constituting markers should be transformed into polygon meshes (constructed of primitives) approximating a sphere. Fixed coordinate system (common to subsequent measurements) is essential. Next step is to transfer of polygon objects (spheres) to subsequent measurements stage with an identical coordinate system.

Table 3 Analysis of point cloud distribution with and without superimposed maps of intensity units (Leica Cyclone view)

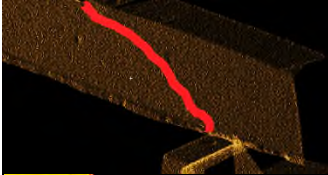
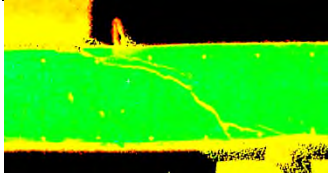
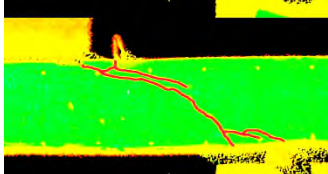
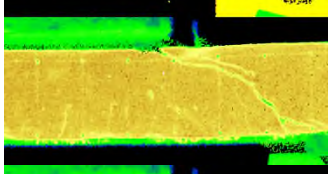
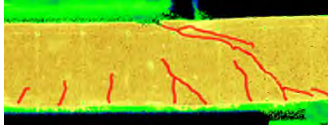
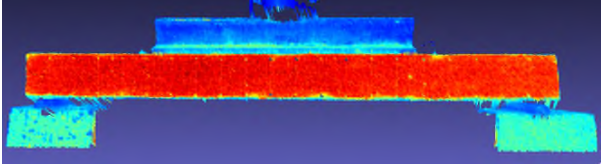
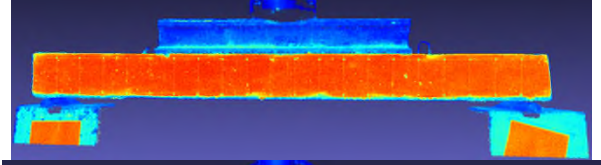
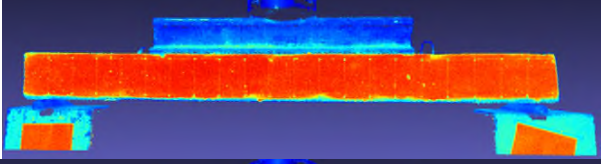
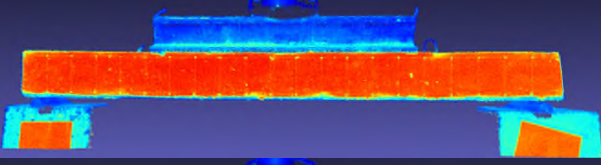
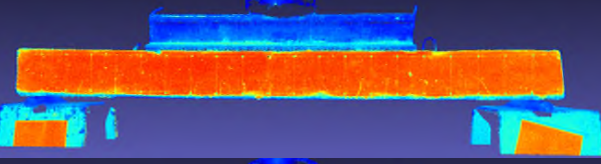
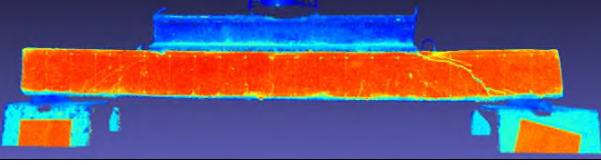
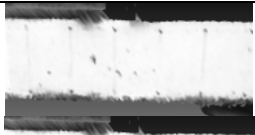
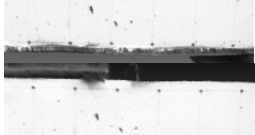
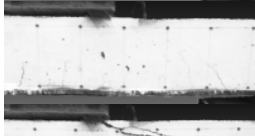
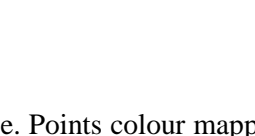
Scheme	MODE OF FAILURE ANALYSIS	
	View of the scan	
No scheme		
No scheme with marked crack		
Multi-Hue/Rainbow		
Multi-Hue/Rainbow with marked cracks		
Topo 3		
Topo 3 with marked cracks		

Table 4 The progress of the beam overloading process (MeshLab view)

Load stage No.	BEAM (SCHEME: MESHLAB RGB)
	View of the scan
1	
2	
3	
4	
5	
6	

However, before the spheres will be transferred to next model space (after load increment), it should be borne in mind that in new model space characteristic tags should be prepared previously in the same way as above. Consequently, as a result, differences in position of the spheres in the same coordinate system should be seen. The difference in spheres coordinates for subsequent stages should be identified as a translation spheres vector, which shows the change of marker position in time. Classical methods of reinforced concrete elements diagnostics, such as dial deflectometer measurement, allow obtaining only vertical displacement value. On the contrary to traditional methods of measurement, spheres translation method allows to identify and measure subtle changes in dimension and location of tags in every direction. One of the most important advantages of this method is a complexity of obtained result. The method is illustrated in the example of the beam geometry changes (Table 2).

Table 5 Comparative analysis of experimental results with the results obtained from TLS scans

No.	BEAM (SCHEME: SAWTOOTH GRAY 8)			View of the scan
	Load [kN]	Cracks in real element	Cracks in virtual model	
1	0.00	-	-	
2	10.00	-	-	
3	30.00	-	-	
4	50.00	A	-	
5	70.00	B	-	
6	90.00	B	B	
7	140.70	C	C	

*A: Flexural (bending) cracks; B: Shear cracks; C: Failure mode onset.

4.2 Colour mapping method

TLS data may be used to study deterioration of concrete surface. Points colour mapping allows tracking cracks propagation in element over time. In the case of reinforced concrete beams, cracks appear in middle part of the beam at failure due to bending, at failure due to shear, cracks occur in support zone. Each point cloud has a certain range of intensity, resulting from maximum and minimum intensity values of sample points. The maximum and minimum values are imposed on marginal colour values of particularized range; this allocation is called a map of intensity. Investigation of point cloud distribution without superimposed map of intensity is not sufficient to monitor structure. During analysis, the authors determined the only faint outline of main failure cracks, which could not constitute a ground for the precise study of this element (Table 3 – rows 1-2). Point cloud with the superimposed map of intensity provides us much more accurate data. Properly applied map of intensity scheme was a significant contribution to extract from TLS data full information of cracks propagation. Imposed intensity map might by modifying, mapping for various point clouds are selected severally by the software. Colour mapping intensity ranges, the so-called “schemes”, can be modified due to particular needs. Change of colour scope in intensity map significantly improve a visibility of cracks propagation (Table 3 – rows 3-6, Table 4).

In order to identify most suitable scheme for research purposes, the analysis was conducted. Compiled data come from the survey of the beam, which reached failure by shear. Information about the geometry of the beam was exported from Leica Cyclone .PTX format and imported into software MeshLab for further analysis. Below authors summarized a couple of schemes that were selected as the best-matching (Table 5).

5. Close range photogrammetry and image analysis of geometry as a tool for verifying experiment with TLS

5.1 Brief introduction

To evaluate results of measurements obtained from TLS authors used the proven method of digital photogrammetry. Photogrammetry involves using the stereo pair of synchronous images. Synchronous images are snapshots taken at one time by two cameras placed in various positions represented by projections centre of the camera lens O_1 and O_2 . Further images were taken with continuous loading. On the cameras imaging planes location of the actual point on the object (P) in

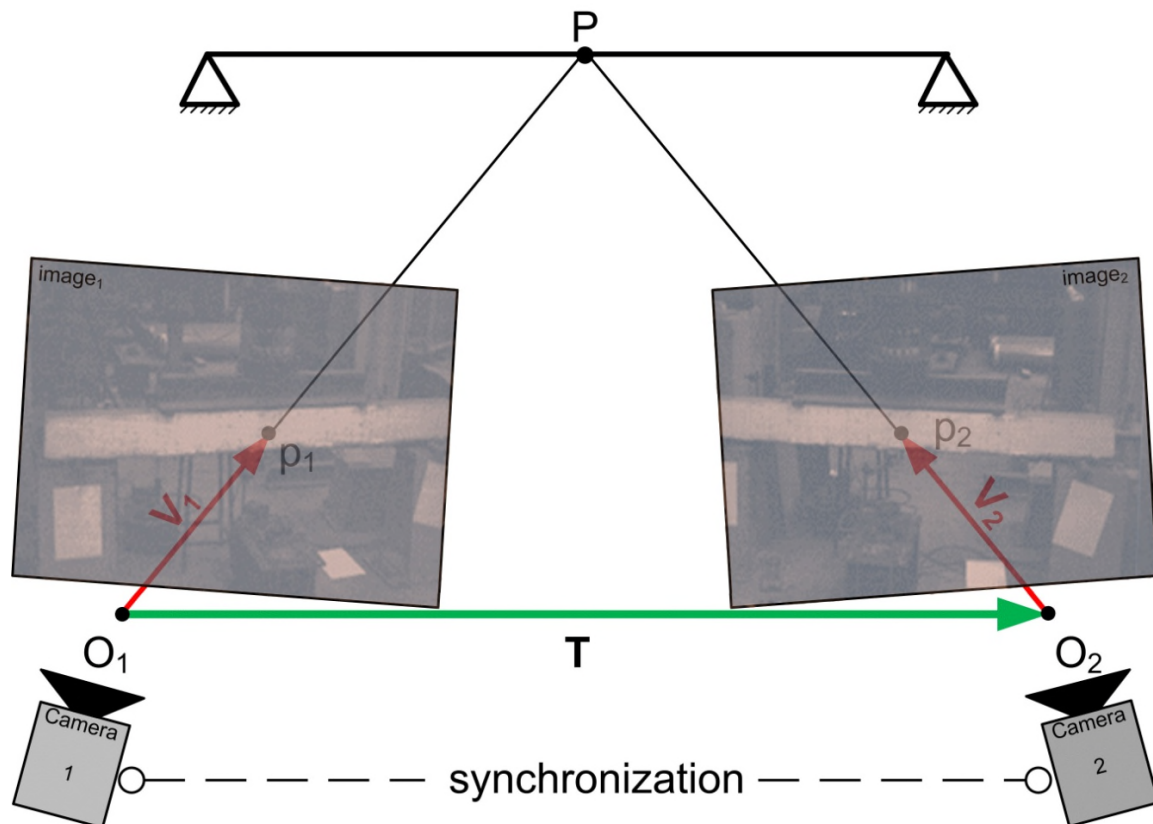


Fig. 6 Photogrammetry registering with use of synchronous digital cameras - scheme

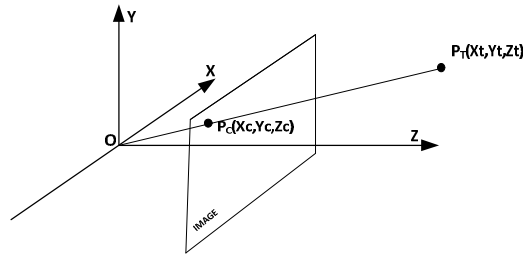


Fig. 7 Theoretical scheme of point P registration on the plane of the image

left (p_1) and right (p_2) image coordinates shall be identified and fixed by camera calibration matrix due to meet the requirements of a stereoscopic model. Obtained representation of points (p_1 , p_2) with camera projections centres (O_1, O_2) shall be combined in order to generate V_1 and V_2 vectors. The offset of a centre of the right camera O_2 in relation to the centre of left the camera O_1 is T vector (Fig. 6).

The combination of these three vectors is positioned on one plane surface. Realization of 3D model reproduction from stereoscopic images by using computer vision is based on a fundamental assumption that two vectors V_1 and V_2 are co-planar. Co-planarity of normalized vectors of points p_1 and p_2 is essential using stereoscopy and photogrammetry (Hartley 1997, Paszotta *et al.* 2010, Kohut *et al.* 2012, Hejmanowska *et al.* 2015).

5.2 Mathematical apparatus—description

After the images acquisition process, point position measurement in pixel coordinates system of each image (X_{pix} , Y_{pix}) can be performed. Later in the mathematical description, general formulas for the cameras will be indicated, the formulas should be applied separately for the camera 1 and camera 2. In theoretical coordinate system, it can be assumed that, spatial position of the point P (X_T , Y_T , Z_T) is known in the camera coordinate system whose centre is located in the middle of camera projection, Z axis runs perpendicular to the plane of the images and is aimed from the centre of the plane projection in the direction of the image surface. X and Y axes coincide with the directions of pixel columns and rows, which forms together with the Z axis clockwise scheme (Fig. 7).

Projected ray which runs through the point P and centre of coordination system intersects the plane of the image in point P_C . Assuming that P_T and P_C points are in homogeneous coordination system and the distance between plane of image and projection centre is f (focal length of camera) the following equation is true

$$\begin{bmatrix} X_C \\ Y_C \\ Z_C \end{bmatrix} = \begin{bmatrix} f & 0 & 0 & 0 \\ 0 & f & 0 & 0 \\ 0 & 0 & 1 & 0 \end{bmatrix} \begin{bmatrix} X_T \\ Y_T \\ Z_T \\ 1 \end{bmatrix} \quad (1)$$

Due to the occurrence of registered images influence of radial and tangential distortions and eccentric position of projection centres (in relation to the image) in the process of obtaining vector components X_C, Y_C should be corrected by using previously determined camera calibration matrix K (Duane 1971, Fryer *et al.* 1986).

$$K = \begin{bmatrix} \alpha_x & \gamma & x_0 \\ 0 & \alpha_y & y_0 \\ 0 & 0 & 1 \end{bmatrix} \quad (2)$$

x_0, y_0 - coordinates of origin point in pixels,

γ - represents the skew coefficient between the x and y-axis, and is often 0,

$\alpha_x = f \cdot m_x, \alpha_y = f \cdot m_y$ - represent focal length in terms of pixels,

m_x, m_y - scale factors relating pixels to distance.

Then corrected coefficients X_C, Y_C, Z_C will be expressed by the formula:

$$\begin{bmatrix} X_C \\ Y_C \\ Z_C \end{bmatrix} = K [I | 0] \begin{bmatrix} X_T \\ X_T \\ Z_T \\ 1 \end{bmatrix} \quad (3)$$

Expression (3) is performed separately for the registrations of point P by camera 1 and by camera 2 using two proper matrices K (respectively for camera 1 and camera 2). Moving on to flat homogeneous, normalized (taking into account notation from Fig. 6) coordinates, it can be assumed that nonlinear vectors V_1, V_2, T are co-planar which is expressed by the equation

$$V_1 \cdot (T \times V_2) = 0 \quad (4)$$

whereas

$$V_1 = \begin{bmatrix} x_1 \\ y_1 \\ 1 \end{bmatrix}; V_2 = \begin{bmatrix} x_2 \\ y_2 \\ 1 \end{bmatrix}; T = \begin{bmatrix} T_1 \\ T_2 \\ T_3 \end{bmatrix} \quad (5)$$

V_1 - normalized vector of point p1 (projected point P on image1) described in camera 1 coordination system.

V_2 - normalized vector of point p2 (projected point P on image2) described in camera 2 coordination system.

T - translation vector of centre of projection of camera 2 in relation to the position of the centre of projection of camera 1.

Implementation of the condition (4) requires presentation of V_2 in camera 1 coordination system. If both the rotation and translation T will be presented as transformations matrices in homogeneous coordinate system, then (4) can be described

$$V_1^T E V_2 = 0 \quad (6)$$

where

$$E = [T]_x R = \begin{bmatrix} E_{11} & E_{12} & E_{13} \\ E_{21} & E_{22} & E_{23} \\ E_{31} & E_{32} & E_{33} \end{bmatrix} \quad (7)$$

moreover

$$R = \begin{bmatrix} R_{11} & R_{12} & R_{13} \\ R_{21} & R_{22} & R_{23} \\ R_{31} & R_{32} & R_{33} \end{bmatrix} \quad (8)$$

is unknown in terms of the value of rotation matrix. E matrix is called an essential matrix and illustrates the interrelation of homologous points in the shared 3D space, expressed in the camera system (using pinhole cameras). When the matrix E is formed as multiplication of translation and rotation matrix includes two equal non-zero singular values and one singular value equal to zero. Constraint (6) can be rewritten as

$$a^T \cdot e = 0 \quad (9)$$

where

$$e = [E_{11} \ E_{12} \ E_{13} \ E_{21} \ E_{22} \ E_{23} \ E_{31} \ E_{32} \ E_{33}]^T \quad (10)$$

and

$$a = [x_1 x_2 \ x_1 y_2 \ x_1 \ y_1 x_2 \ y_1 y_2 \ y_1 \ x_2 \ y_2 \ 1]^T \quad (11)$$

When you have given a set of n corresponding image points you have matrix A

$$A = [a_1 \ a_2 \ \dots \ a_n]^T \quad (12)$$

This gives finally linear equation

$$Ae = 0 \quad (13)$$

and the possibility to obtain the vector e and matrix Eq. (7).

We make the additional constraints: $\|e\| = 1$, $E_{33} = 1$ and solving (13) as a linear least squares minimization problem – it needs at least 8 point matches on two images.

Errors of measurement and point identification result that this assumption is not entirely numerically correct. By adopting a substitute, for the matrix E, matrix E'

$$E' = UDV^T \quad (14)$$

such that

$$D = \text{diag}(1,1,0) \quad (15)$$

and assuming matrix $W = \begin{bmatrix} 0 & -1 & 0 \\ 1 & 0 & 0 \\ 0 & 0 & 1 \end{bmatrix}$ it is possible to separate matrices $[T]_x$ and R from E'.

Each of them adopts one of two values thus giving the four possible solutions of matrices combination $[T]_x$ and R

$$[T]_{x1} = \begin{bmatrix} U_{31} \\ U_{32} \\ U_{33} \end{bmatrix} \quad \text{or} \quad [T]_{x2} = -\begin{bmatrix} U_{31} \\ U_{32} \\ U_{33} \end{bmatrix} \quad (16)$$

$$R_1 = UWV^T \quad \text{or} \quad R_2 = UW^T V^T \quad (17)$$

All pairs of values ($[T]_x$, R) should be examined and the right one shall be chosen. It may be p_1 and p_2 imaging was generated as a result of projections determined by M_1 and M_2 matrices (size of 3×4) of P on the imaging planes of camera 1 and camera 2 (Fig. 6) assumed that

$$p_1 = M_1 P \quad \text{or} \quad p_2 = M_2 P \quad (18)$$

$$M_1 = \begin{bmatrix} 1 & 0 & 0 & 0 \\ 0 & 1 & 0 & 0 \\ 0 & 0 & 1 & 0 \end{bmatrix} \quad (19)$$

whereas

$$M_2 = H^{-1} \quad (20)$$

moreover

$$H = \begin{bmatrix} R_i & [T]_{xj} \\ 0 & 1 \end{bmatrix} \quad \text{for } i=1..2, j=1..2 \quad (21)$$

then the following system of equations is true

$$\begin{cases} p_1 \times M_1 P = 0 \\ p_2 \times M_2 P = 0 \end{cases} = \begin{cases} [p_1]_x M_1 P = 0 \\ [p_2]_x M_2 P = 0 \end{cases} \quad (22)$$

which can be symbolically expressed as

$$BP = 0 \quad (23)$$

P vector may be calculated by subjecting B matrix to SVD decomposition

$$B = USV^T \quad (24)$$

P vector will be equal to the last column of the V matrix. After its normalization, it is necessary to

calculate the position of P point with respect to the camera 2, i.e. P'

$$P' = M_2 P \quad (25)$$

If the components of the vectors P and P' are respectively upstream camera 1 and camera 2, this pair of $[T]_x$ and R (the only one among the four) is correct and they are used in formulas (18) to calculate the coordinates in the model system of all points measured in the image. The model system is a system in which there is an isometry of points position in relation to their equivalents from the real world but the scale is not determined. The scaling effect may be achieved by pointing, at least two points from the point cloud (distance between this two points has to be known variable). The model might be also levelled, by using, at least three non-collinear points from the point cloud. Nowadays on the market there is a wide range of solutions based on photogrammetry and Computer Vision - eg. 3D Scanner ARAMIS, adaptations of Microsoft Kinect or Microsoft Kinect 2.0 and even cameras in smartphones, which allows to obtain point cloud model (Goszczynska B *et al.* 2015, Nagrodzka-Godycka *et al.* 2015, Qi *et al.* 2014). Photogrammetric measurement solution presented in this paper has been implemented and coded as a standalone desktop application (Janowski *et al.* 2014.1). This standalone application uses synchronous photographs as an input. In presented solution, the algorithm applied to the application has been improved in the term of accuracy and effectiveness. Embedded solution is consistent with the general theory described in the literature (Hartley 1997 W. Wang *et al.* 2000). Mentioned method has been used as a verification of the measurement results obtained from TLS. Scaling was performed using data from TLS and actual measurements. The accuracy obtained using digital photogrammetry methods are much higher than measurements using point clouds (Janowski *et al.* 2005, Janowski *et al.* 2014.2).

6. Summary and conclusions

The leading goal of this particular study was to determine whether and how TLS might be used in diagnostics of reinforced concrete elements. Authors show that this technology can be used to register a deformation process, examine and measure geometry of reinforced concrete (RC) beams. However, all of these advantages have certain restrictions. TLS boundary conditions and limitations shall designate a level of its potential applications in diagnostic of RC element. Through fuse of photogrammetry and photogrammetrically prepared synchronous photos, it has been established that TLS might be used for the failure analysis of reinforced concrete beams and other concrete elements. Prerequisites described in section 3 designate usability areas of TLS, authors conclude that links usage for signal tags locating is incorrect because it leads to dilution of global coordination system. Signal tags lead themselves to micro-shifts which in macro scope geodesy measurements are meaningless, but they are crucial in deformation measurement. Exclusion of inaccuracies associated with scans bonding and adverse albedo (fraction of reflected shortwave radiation) of concrete surface requires that previously scanned the object and the scanner had to be in the same local coordination system. The position of the scanner during measurement process cannot be changed in relation to the scanned element. At the stage of element preparation, it is recommended to engobe scanned surface in order to provide better contrast between the surface of concrete and expanding cracks, white colour reflects light much

more intense than different colours. Resolution of measurement have an impact on the density of point cloud, scan resolution should be predefined before measurement and maintained at fairly high level. Data from TLS about cracks propagation enable to infer which mode of failure occurred, but only in the pre-critical stage. This technology allows creating full three-dimensional, specific, virtual model of the structure with full operability. An important advantage of laser scanning is a speed of measurements, the standard scan may be formed even in 3 minutes. Furthermore, objects might be investigated without any physical contact and laser scanning can penetrate inaccessible areas. The most important advantage of TLS over the classical methods of deformation measurement is complexity and immersion of obtained results.

References

- Bencardino, F. and Condello, A. (2014), "Experimental study and numerical investigation of behavior of RC beams strengthened with steel reinforced grout", *Comput. Concrete*, **14**(6), 711-725.
- Błaszczak-Bąk, W., Janowski, A., Kamiński, W. and Rapiński, J. (2015), "Application of the Msplit method for filtering airborne laser scanning data-sets to estimate digital terrain models", *Int. J. Remote Sens.*, **36**(9), 2421-2437.
- Daliga, K. and Kuralowicz, Z. (2016), "Examination method of the effect of the incidence angle of laser beam on distance measurement accuracy to surfaces with different colour and roughness", *Boletim de Ciencias Geodesicas*, **22**(3)
- Dias-da-Costa, D., Valença, J. and do Carmo, R.N.F. (2014), "Curvature assessment of reinforced concrete beams using photogrammetric techniques", *Mater. Struct.*, **47**(10), 1745-1760.
- Duane, C.B. (1971), "Close-range camera calibration", *Photogramm. Eng.*, **37**(8), 855-866.
- Fryer, J.G. and Brown, D.C. (1986), "Lens distortion for close-range photogrammetry", *Photogramm. Eng. Remote Sens.*, **52**(1), 51-58.
- Godycki-Ćwirko, T. (1992), "Crack morphology in concrete structures", *Sci. Study*, **13**, 149.
- González-Aguilera, D., Gómez-Lahoz, J. and Sánchez, J. (2008), "A new approach for structural monitoring of large dams with a three-dimensional laser scanner", *Sensors*, **8**(9), 5866-5883.
- Gordon, S.J. and Lichti, D.D. (2007), "Modeling terrestrial laser scanner data for precise structural deformation measurement", *J. Survey. Eng.*, **133**(2), 72-80.
- Goszczyńska, B., Świt, G. and Trąmpczyński, W. (2015), "Analysis of the microcracking process with the Acoustic Emission method with respect to the service life of reinforced concrete structures with the example of the RC beams", *Bull. Polish Academy Sci. Tech.*, **63**(1), 55-63.
- Hartley, R.I. (1997), "In defense of the eight-point algorithm. Pattern analysis and machine intelligence", *Proceedings of the IEEE Transactions on*, **19**(6), 580-593.
- Hejmanowska, B., Przyborski, M., Pyka, K. and Pырchla, J. (2015), "Modern remote sensing and the challenges facing education systems in terms of its teaching", *Proceedings of the 7th International Conference on Education and New Learning Technologies*, 6549-6558, Barcelona, Spain
- Janowski, A. and Rapinski, J. (2013), "M-split estimation in laser scanning data modeling", *J. Indian Soc. Remote Sens.*, **41**(1), 15-19.
- Janowski, A. and Szulwic, J. (2014), "Synchronic digital stereophotography and photogrammetric analyses in monitoring the flow of liquids in open channels", *Proceedings of the 9th ICEE*, 2029-7092.
- Janowski, A., Nagrodzka-Godycka, K., Szulwic, J. and Ziółkowski, P. (2014), "Modes of failure analysis in reinforced concrete beam using laser scanning and synchro-photogrammetry", *Proceedings of the 2nd Int. Conference on Adv. Civil, Struct. Envir. Eng.*, 16-20.
- Janowski, A., Sawicki, P. and Szulwic, J. (2005), "Advanced 3D visualization of an architectural object in the OpenGL standard", *Int. Arch. Photogramm., Remote Sens. Spatial Inform. Sci.*, **36**(2).
- Kohut, P., Mikrut, S., Pyka, S., Tokarczyk, R. and Uhl, T. (2012), "Research on the prototype of rail

- clearance measurement system”, *Proceedings of the 22nd Congress of the International-Society-for-Photogrammetry-and-Remote-Sensing*, 25 Aug.–01 Sep. 2012, Melbourne, Australia. Book Series: International Archives of the Photogrammetry Remote Sensing and Spatial Information Sciences, **39**, B4.
- Koken, A., Koroglu, M.A., Karabork, H. and Ceylan, A. (2014), “Photogrammetric approach in determining beam-column connection deformations”, *Boletim de Ciências Geodésicas*, **20**(3), 720-733.
- Kopańska, A. and Nagrodzka-Godycka, K. (2016), “The influence of reinforcement on load carrying capacity and cracking of the reinforced concrete deep beam joint”, *Eng. Struct.*, **107**, 23-33.
- Kwak, E., Datchev, I., Habib, A., El-Badry, M. and Hughes, C. (2013), “Precise photogrammetric reconstruction using model-based image fitting for 3D beam deformation monitoring”, *J. Survey. Eng.*, **139**(3), 143-155.
- Lichti, D.D., Jantsch, S., El-Halawany, S.I., Lahamy, H., Chow, J., Chan, T.O. and El-Badry, M. (2011), “Structural deflection measurement with a range camera”, *J. Survey. Eng.*, **138**(2), 66-76.
- Moradi-Marani, F., Rivard, P., Lamarche, C.P. and Kodjo, S.A. (2014), “Evaluating the damage in reinforced concrete slabs under bending test with the energy of ultrasonic waves”, *Constr. Build. Mater.*, **73**, 663-673.
- Nagrodzka-Godycka, K., Szulwic, J. and Ziółkowski, P. (2014), “The method of analysis of damage reinforced concrete beams using terrestrial laser scanning”, *Proceedings of the 14th SGEM GeoConference on Informatics, Geoinformatics and Remote Sensing*, **3**, 335-342.
- Nagrodzka-Godycka, K., Szulwic, J. and Ziółkowski, P. (2015), “Method of selective fading as a educational tool to study the behaviour of prestressed concrete elements under excess loading”, *Proceedings of the ICERI2015*, 472-479
- Olsen, M.J., Kuester, F., Chang, B.J. and Hutchinson, T.C. (2009), “Terrestrial laser scanning-based structural damage assessment”, *J. Comput. Civil Eng.*, **24**(3), 264-272.
- Paszotta, Z. and Szumilo, M. (2010), “A web-based approach for online digital terrain model and orthoimage generation”, *Proceedings of the 1st International Workshop on pervasive Web Mapping, Geoprocessing and Services*, 26-27.
- Qi, X., Lichti, D., El-Badry, M., Chow, J. and Ang, K. (2014), “Vertical dynamic deflection measurement in concrete beams with the Microsoft kinect”, *Sensors*, **14**(2), 3293-3307.
- Rucka, M. and Wilde, K. (2013), “Experimental study on ultrasonic monitoring of splitting failure in reinforced concrete”, *J. Nondestr. Eval.*, **32**(4), 372-383.
- Szulwic, J., Burdziakowski, P., Janowski, A., Przyborski, M., Tysiąc, P., Wojtowicz, A.,... and Matysik, M. (2015), “Maritime laser scanning as the source for spatial data”, *Polish Maritime Res.*, **22**(4), 9-14.
- Teza, G., Galgaro, A. and Moro, F. (2009), “Contactless recognition of concrete surface damage from laser scanning and curvature computation”, *NDT & E Int.*, **42**(4), 240-249.
- Wang, W. and Tsui, H.T. (2000), “A SVD decomposition of essential matrix with eight solutions for the relative positions of two perspective cameras”, *Proceedings 15th International Conference Pattern Recognition*, **1**, 362-365.
- Windisch A. (1988), “Das Modell der charakteristischen Bruchguerschnitte”, *Beton und Stahlbetonbau*, **83**(9), 251-255.